

Spin-gapped metals: A novel class of materials - the case of semi-Heusler compounds

E. Şaşıoğlu^{1,*}, M. Tas^{2,†}, S. Ghosh³, W. Beida⁴, B. Sanyal^{3,‡}, S. Blügel⁴, I. Mertig¹, and I. Galanakis^{5,§}

¹*Institute of Physics, Martin Luther University Halle-Wittenberg, 06120 Halle (Saale), Germany*

²*Department of Physics, Gebze Technical University, 41400 Kocaeli, Turkey*

³*Department of Physics and Astronomy, Uppsala University, 75120 Uppsala, Sweden*

⁴*Peter Grünberg Institut, Forschungszentrum Jülich and JARA, 52425 Jülich, Germany*

⁵*Department of Materials Science, School of Natural Sciences, University of Patras, GR-26504 Patras, Greece*

(Dated: March 5, 2024)

Gapped metals, a recently discovered new class of materials, possess a band gap slightly above or below the Fermi level. These materials are intrinsic p- or n-type semiconductors eliminating the need for extrinsic doping. Inspired by this concept, we propose the so-called "spin-gapped metals" exhibiting intrinsic p- or n-type behavior for each spin channel independently. Their properties would be similar to the dilute magnetic semiconductors eliminating the requirement for transition metal doping. Here, we demonstrate this novel concept in semi-Heusler compounds using first-principles electronic band structure calculations. We comprehensively analyze their electronic and magnetic properties, paving the way for novel technological applications of Heusler compounds.

Introduction: An essential hurdle in materials science involves uncovering materials possessing unique characteristics that can bolster device performance. Thermoelectricity, which involves converting heat into electricity via the Seebeck effect, stands as a pivotal phenomenon in contemporary technology, enabling the harnessing of waste heat from both industrial and household processes [1, 2]. While doped semiconductors are traditionally favored for thermoelectric applications, recent suggestions propose a new category of metals termed "gapped metals" as potential substitutes for doped semiconductors [3–5]. As illustrated in Fig. 1(a-c), the density of states (DOS) for these gapped metals reveals a semiconductor-like gap, which distinguishes them from conventional metals. Specifically, the Fermi level intersects either the valence band, resulting in an excess of holes (p-type gapped metals), or the conduction band, leading to an excess of electrons (n-type gapped metals). This class of metals has the potential to supplant doped semiconductors in various applications without the necessity for additional doping.

Expanding the concept of gapped metals to encompass magnetic materials could involve introducing the term "spin-gapped metals", indicating differing behaviors in the electronic band structures regarding spin. Such an extension would result in a diverse range of behaviors stemming from the distinct characteristics of each metal. Presented in Fig. 1(d-f) are seven distinct scenarios illustrating this concept. By combining n- or p-type gapped metallic behavior for the spin-up electronic band structure with various behaviors such as normal metallic, typical semiconducting, or n(p)-type gapped metallic behavior in the spin-down electronic band structure, a broader range of implications for technology applications could be

achieved. Analogous to how gapped metals are seen as counterparts to doped semiconductors, one might view spin-gapped metals as counterparts to dilute magnetic semiconductors [6–9], such as Mn-doped GaAs, without requiring the incorporation of magnetic atoms through doping.

The Heusler compounds [10, 11] constitute a vast family of intermetallic compounds, currently comprising over 2000 members [12–14]. Within this family, numerous novel behaviors have been both experimentally and computationally identified, rendering them appealing for a wide array of technological applications. These behaviors include half-metallicity [15], spin-gapless semiconducting behavior [16, 17], spin-filtering [18], and more. Their adaptability regarding element substitution drives ongoing research in this field, and extended databases were built using the first-principles calculations resulting in the prediction of hundreds of new Heusler compounds which were later grown experimentally [15, 17, 19–26]. Among these compounds, the so-called 18-valence electrons semi-(or half-)Heusler compounds, such as CoTiSb, FeVSb, or NiTiSn, are renowned semiconductors exhibiting remarkably high-temperature thermoelectric properties [19, 27–33]. Alternative approaches, like cation-deficient 19-valence electron semi-Heusler compounds [34] or Rubik’s-cube-like Heusler semiconductors [35], have been proposed to tailor thermoelectric properties as desired. In seeking spin-gapped metals within the semi-Heusler compounds, deviating from the 18-valence electrons semiconducting Heusler compounds seems a logical step. To pursue this objective, we conducted a search in the Open Quantum Materials Database (OQMD) [36] and identified 33 semi-Heusler compounds, as outlined in Table I. These compounds typically possess 17 or 19 valence electrons per unit cell, though some exceptions with 16, 20, or 21 valence electrons exist. Our initial criterion for selecting compounds for the study was their formation energy, E_{form} , which we aimed to be negative, with a few exceptions like FeVSn and CuVSb included for completeness, as their values were close to zero de-

* ersoy.sasioglu@physik.uni-halle.de

† murat.tas@gtu.edu.tr

‡ biplab.sanyal@physics.uu.se

§ galanakis@upatras.gr

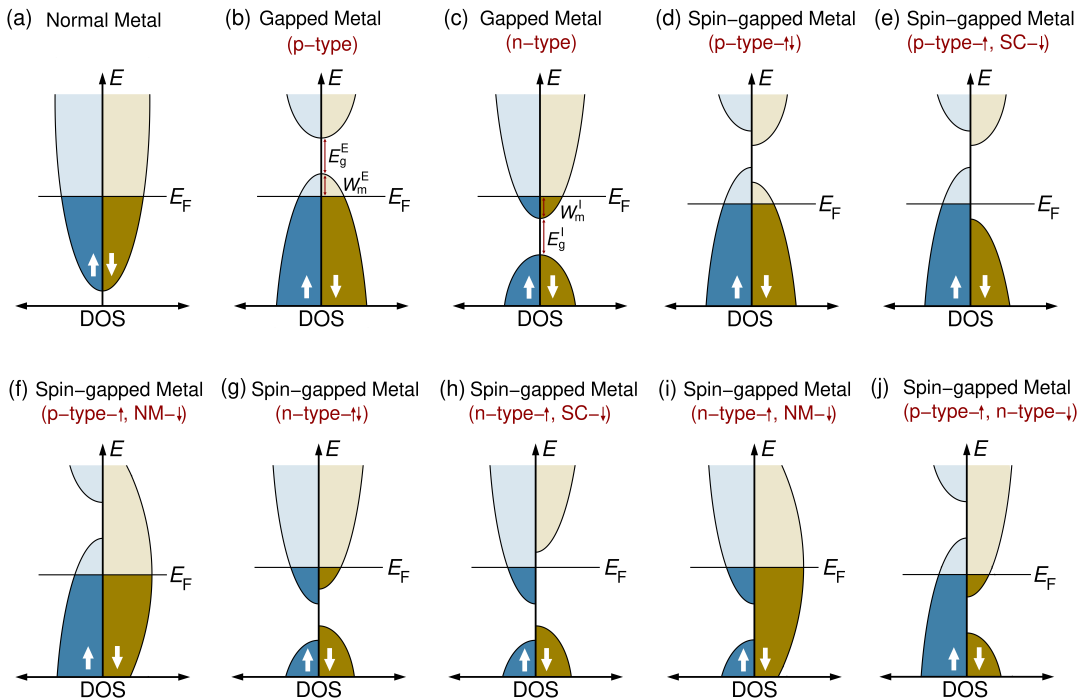


FIG. 1. Schematic representation of the density of states (DOS) of a normal metal (a), gapped metals (b-c), and spin-gapped metals (d-j). The arrows represent the two possible spin directions. The horizontal line depicts the Fermi level E_F . NM stands for normal-metal and SC for semiconductor.

spite being positive. However, negative E_{form} alone does not guarantee stability. The convex hull distance ΔE_{con} , which represents the energy difference between the studied structure and the most stable phase or a mixture of phases, is also crucial. Typically, values less than 0.2 eV/atom are desired to facilitate the growth of a material in a metastable form, such as a thin film or a nanostructure. All materials selected from OQMD for our study exhibit ΔE_{con} values less than the cutoff of 0.2 eV/atom, except for CuVSb, which has a value of 0.24 eV/atom. The formation and convex hull distance energies from OQMD are detailed in Table I.

Computational details: The bulk semi-Heusler compounds XYZ crystallize in the cubic $C1_b$ lattice structures (see figure 2 in Ref. 15). The space group is the $F\bar{4}3m$ and actually consists of four interpenetrating f.c.c. sublattices; one is empty and the other three are occupied by the X , Y , and Z atoms. The unit cell is an f.c.c. one with three atoms as a basis along the long diagonal of the cube: X at (000), Y at $(\frac{1}{4}\frac{1}{4}\frac{1}{4})$ and Z at $(\frac{3}{4}\frac{3}{4}\frac{3}{4})$ in Wyckoff coordinates. We adopted the lattice constants calculated in the Open Quantum Materials Database (OQMD) for all thirty-three materials [36], and we present them in the second column in Table I. Our tests show that the lattice constants presented in OQMD, where the Perdew-Burke-Ernzerhof (PBE) functional has been used for the exchange-correlation potential [37], differ less than 1 % from the PBE equilibrium ones calculated with the electronic band structure methods employed in the current study.

The ground-state first-principles electronic band-structure calculations for all studied compounds were carried out using the QUANTUMATK software package [38, 39]. We use linear combinations of atomic orbitals (LCAO) as a basis set together with norm-conserving PseudoDojo pseudopotentials [40]. The PBE parameterization to the generalized-gradient-approximation of the exchange-correlation potential is employed [37]. Note that due to the metallic character of the compounds under study, the GGA provides a more accurate description of the ground state properties concerning more complex hybrid functionals [33, 41]. For determination of the ground-state properties of the bulk compounds, we use a $16 \times 16 \times 16$ Monkhorst-Pack \mathbf{k} -point grid [42].

For the effective Coulomb interaction parameters (Hubbard U and Hund exchange J in Table II) we followed the same *ab-initio* method already employed in Refs. 43 and 44 for the Mn-based full Heusler compounds. First, we performed non-magnetic ground state calculations using the full-potential linearized augmented plane waves (FLAPW) method as implemented in the FLEUR code [45]. Then we employed the SPEX code [46] to calculate the effective Coulomb parameters within the constrained random-phase-approximation (cRPA). The calculated U and J are then used to determine the Stoner parameter $I = (U + 6J)/5$ [47]. Note that in Ref. 47 the authors have shown that electron correlation reduces I by roughly 40% and thus one has to scale down the Stoner parameter by a factor $\alpha = 0.6$.

To calculate the Curie temperature for the spin-gapped

TABLE I. Lattice constants a_0 , valence electron number Z_T , sublattice and total magnetic moments, spin polarization at the Fermi level (see text for definition), spin gap type per spin direction, the distance of the Fermi level from the edge of the band which it crosses $W_m^{I,E(\uparrow/\downarrow)}$ (see text for more details), energy gap per spin direction $E_g^{I,E(\uparrow/\downarrow)}$, formation energy (E_{form}), convex hull distance energy (ΔE_{con}) in parenthesis, and calculated Curie temperatures for the compounds under study. The a_0 , E_{form} and ΔE_{con} values are taken from the Open Quantum Materials Database [36].

Compound XYZ	a_0 (Å)	Z_T	m_X (μ_B)	m_Y (μ_B)	m_{total} (μ_B)	SP (%)	Spin gap type	$W_m^{I,E(\uparrow/\downarrow)}$ (eV)	$E_g^{I,E(\uparrow/\downarrow)}$ (eV)	E_{form} (E_{con}) (eV/at.)	T_C (K)
Spin-gapped metals											
FeZrSn	6.24	16	-2.03	0.18	-1.90	64	p-type- \uparrow /p-type- \downarrow	1.14/0.17	0.74/0.55	-0.22 (0.19)	74
FeHfSn	6.19	16	-1.86	0.17	-1.74	28	p-type- \uparrow /p-type- \downarrow	1.09/0.31	1.18/0.55	-0.18 (0.16)	98
FeTiSb	5.94	17	-1.45	0.53	-0.95	68	p-type- \uparrow /p-type- \downarrow	0.58/0.12	0.47/0.76	-0.39 (0.04)	220
FeZrSb	6.15	17	-1.34	0.34	-1.00	100	p-type- \uparrow /SC- \downarrow	0.64/	0.90/	-0.45 (0.03)	255
FeHfSb	6.11	17	-1.26	0.27	-1.00	100	p-type- \uparrow /SC- \downarrow	0.60/	1.28/	-0.39 (0.00)	240
FeVSn	5.87	17	-1.85	1.03	-0.88	36	NM- \uparrow /p-type- \downarrow	/0.15	/0.59	0.06 (0.18)	215
FeNbSn	6.00	17	-1.38	0.40	-1.00	100	p-type- \uparrow /SC- \downarrow	0.70/	0.16/	-0.10 (0.06)	220
FeTaSn	5.99	17	-1.29	0.32	-1.00	100	p-type- \uparrow /SC- \downarrow	0.70/	0.56/	-0.06 (0.09)	225
CoTiSn	5.93	17	-0.42	-0.45	-0.94	74	p-type- \uparrow /p-type- \downarrow	0.37/0.06	0.94/0.84	-0.38 (0.07)	70
CoZrSn	6.15	17	-0.67	-0.18	-0.95	81	p-type- \uparrow /p-type- \downarrow	0.41/0.09	0.97/0.74	-0.46 (0.05)	80
CoHfSn	6.11	17	-0.55	-0.15	-0.79	66	p-type- \uparrow /p-type- \downarrow	0.38/0.24	1.02/0.71	-0.43 (0.04)	85
RhTiSn	6.17	17	-0.07	-0.73	-0.87	70	p-type- \uparrow /p-type- \downarrow	0.56/0.09	0.63/0.65	-0.60 (0.06)	140
IrTiSn	6.20	17	-0.08	-0.61	-0.76	33	p-type- \uparrow /p-type- \downarrow	0.45/0.13	0.71/0.67	-0.61 (0.02)	100
NiTiIn	5.99	17	-0.04	-0.81	-0.97	97	p-type- \uparrow /p-type- \downarrow	0.51/0.01	0.30/0.49	-0.18 (0.18)	170
NiZrIn	6.22	17	-0.11	-0.31	-0.55	53	p-type- \uparrow /p-type- \downarrow	0.49/0.34	0.30/0.30	-0.31 (0.12)	5
PdTiIn	6.23	17	-0.03	-0.87	-0.99	99	p-type- \uparrow /p-type- \downarrow	0.50/0.04	0.38/0.45	-0.31 (0.15)	160
PtTiIn	6.24	17	-0.04	-0.84	-1.00	100	p-type- \uparrow /SC- \downarrow	0.45/	0.78/	-0.56 (0.10)	200
CoVsb	5.81	19	-0.33	1.41	1.00	100	n-type- \uparrow /SC- \downarrow	0.79/	0.35/	-0.19 (0.07)	325
RhVsb	6.07	19	-0.21	1.33	1.00	100	n-type- \uparrow /SC- \downarrow	0.87/	0.25/	-0.31 (0.10)	180
IrVsb	6.07	19	-0.21	1.26	1.00	100	n-type- \uparrow /SC- \downarrow	0.99/	0.28/	-0.29 (0.15)	225
PdTiSb	6.24	19	-0.04	0.98	0.89	87	n-type- \uparrow /n-type- \downarrow	0.59/0.19	0.49/0.41	-0.51 (0.09)	220
PtTiSb	6.26	19	-0.05	1.05	0.99	93	n-type- \uparrow /n-type- \downarrow	0.53/0.02	0.74/0.78	-0.65 (0.11)	178
NiVSn	5.87	19	-0.03	1.15	1.00	100	n-type- \uparrow /SC- \downarrow	0.41/	0.67/	-0.08 (0.15)	117
NiVsb	5.88	20	0.03	2.12	2.00	100	n-type- \uparrow /SC- \downarrow	0.68/	0.80/	-0.12 (0.13)	670
CuVsb	6.06	21	0.04	3.04	2.95	40	n-type- \uparrow /NM- \downarrow	1.44/	0.15/	0.21 (0.24)	635
Gapped metals											
NiHfIn	6.16	17	0.00	0.00	0.00	0	p-type- \uparrow /p-type- \downarrow	0.45/0.45	0.32/0.32	-0.26 (0.17)	
CoNbSb	5.97	19	0.00	0.00	0.00	0	n-type- \uparrow /n-type- \downarrow	0.57/0.57	0.95/0.95	-0.22 (0.15)	
CoTaSb	5.96	19	0.00	0.00	0.00	0	n-type- \uparrow /n-type- \downarrow	0.53/0.53	1.17/1.17	-0.14 (0.20)	
NiTiSb	5.93	19	0.00	0.00	0.00	0	n-type- \uparrow /n-type- \downarrow	0.69/0.69	0.61/0.61	-0.52 (0.05)	
NiZrSb	6.15	19	0.00	0.00	0.00	0	n-type- \uparrow /n-type- \downarrow	0.88/0.88	0.75/0.75	-0.62 (0.03)	
NiHfSb	6.10	19	0.00	0.00	0.00	0	n-type- \uparrow /n-type- \downarrow	0.96/0.96	0.67/0.67	-0.53 (0.06)	
NiNbSn	6.00	19	0.00	0.00	0.00	0	n-type- \uparrow /n-type- \downarrow	0.73/0.73	0.88/0.88	-0.19 (0.09)	
NiTaSn	5.99	19	0.00	0.00	0.00	0	n-type- \uparrow /n-type- \downarrow	0.87/0.87	0.83/0.83	-0.11 (0.13)	

metals in Table I, we employed a Monte-Carlo technique similar to the study of spin-gapless semiconductors in Ref. 48. First, as in Ref [32], the Heisenberg exchange constants are calculated by employing the Liechtenstein formalism [49] within the full-potential linear muffin-tin orbital (FP-LMTO) code RSPt [50]. Then the calculated exchange parameters are used as input for the Monte-Carlo technique to calculate the magnetic susceptibility [48]. The Curie temperature is determined by the divergence of the susceptibility (see [48] for details).

Finally, we should note that according to our tests, all three QuantumATK, FLAPW, and FP-LMTO methods provide very similar electronic structure for the systems under study.

Results and discussion: In the first step of our study, we have chosen thirty-three semi-Heusler compounds

as discussed in preceding section and calculated their ground state properties. In Table I we have compiled our results. We have eight compounds that are non-magnetic and belong to the gapped metals. Among them, only NiHfIn has 17 valence electrons per unit cell while the other seven have 19 valence electrons. Since the 18 valence electrons compounds are semiconductors, one would expect NiHfIn to be a p-type gapped metal with the Fermi level crossing the valence band and the rest n-type gapped metals with the Fermi level crossing the conduction band. Our calculated band structures confirm these predictions as shown in Table I. In Table I we also include the distance of the Fermi level from the edge of the band which it crosses, $W_m^{I,E(\uparrow/\downarrow)}$, *i.e.*, for the n-type case, it is the distance from the conduction band minimum and for the p-type case the distance from the valence band maximum.

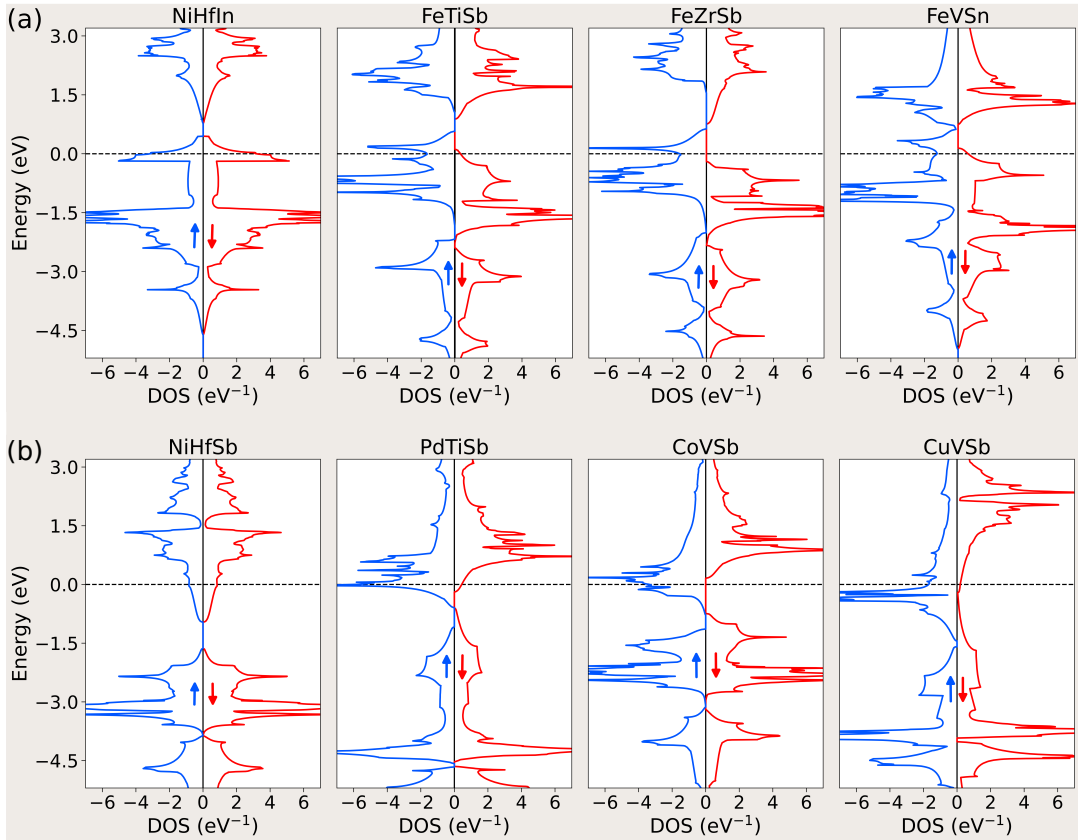


FIG. 2. Spin-resolved total density of states for selected gapped and spin-gapped Heusler compounds. The zero energy corresponds to the Fermi level. Arrows depict the two spin directions.

The $W_m^{I,E(\uparrow/\downarrow)}$ value is followed by the $E_g^{I,E(\uparrow/\downarrow)}$ one which is the width of the energy gap. For each quantity, we provide two values separated by a slash corresponding to the two spin directions. As it is obvious for the gapped metals the values for both spin directions are identical. Both $W_m^{I,E(\uparrow/\downarrow)}$ and $E_g^{I,E(\uparrow/\downarrow)}$ values are less than 1 eV and are comparable.

The rest twenty five compounds under study are spin-gapped materials as shown in Table I. The ones with less than 18 valence electrons per unit cell have negative total spin magnetic moments per unit cell and are p-type spin-gapped metals. The compounds with more than 18 valence electrons, on the other hand, have positive total spin magnetic moments and are n-type spin-gapped metals. All n-type (p-type) spin-gapped metals are not identical concerning their density of states. As shown in Table I there are several cases where the two spin band structures have a different character, *i.e.*, the one spin channel presents either a normal metallic (NM) or semiconducting (SC) behavior while the other spin channel presents a n(p)-type spin-gapped metallic behavior. To make this clear, in Fig. 2 we have gathered the total DOS for some selected compounds and compared them with the schematic representations in Fig. 1. NiHfIn and NiHfSn are p-type and n-type gapped metals, respectively. FeTiSb presents p-type spin-gapped

metallic behavior for both spin directions. FeZrSb and FeVSn present p-type behavior for one spin direction and semiconducting (normal metallic) for the other. Similarly, PdTiSb, CoVSb and CuVSb present n-type spin-gapped metallic behavior for one spin direction and n-type/semiconducting/normal-metallic behavior for the other spin direction. None of the studied compounds presents an electronic band structure similar to the j panel in Fig. 1, where one spin-band is n-type and the other p-type. One could envisage that this behavior can be identified in another class of Heusler compounds like the equiatomic quaternary Heuslers since several of them are type-II spin-gapless semiconductors [51, 52]. Actually in Ref. 53 (see figure 1), MnVTiAs compound combines a p-type gapped metallic behavior for the spin-up band structure with an n-type gapped metallic behavior for the spin-down electronic band structure. In this article, this behavior was referred to as "indirect spin-gapless semiconductors" since the concept of "spin-gapped metals" was not known.

In Table I, we have also included the atom-resolved spin magnetic moments for the two transition atoms in each compound, the spin-polarization SP at the Fermi level, and the Curie temperature. The atomic spin magnetic moments do not present any peculiarity. The transition metal atoms from Ti to Co are the ones carrying

TABLE II. The d -orbitals, effective Coulomb interaction parameters (Hubbard U and Hund exchange J) between the localized d -orbitals, the Stoner parameter I , and the total density of states at the Fermi level ($N(E_F)$). The next columns present the product $I \cdot N(E_F)$ and the same product multiplied by the $\alpha = 0.6$ coefficient (see text for details). Note that the slash separates the values for the two transition metal atoms X and Y in the chemical formula of the compound. The values in the third to eighth columns have been obtained using non-spin polarized calculations.

XYZ	Orbitals	U (eV)	J (eV)	I (eV)	$N(E_F)$ (eV $^{-1}$)	$I \cdot N(E_F)$	$\alpha \cdot I \cdot N(E_F)$
Spin-gapped metals							
FeZrSn	3d/4d	1.93/1.50	0.88/0.39	1.44/0.76	1.50/1.21	2.16/0.92	1.30/0.55
FeHfSn	3d/5d	2.08/1.40	0.89/0.36	1.48/0.71	1.28/0.76	1.84/0.54	1.14/0.32
FeTiSb	3d/3d	2.42/2.65	0.85/0.61	1.50/1.27	1.72/1.42	2.58/1.80	1.55/1.08
FeZrSb	3d/4d	2.73/1.75	0.90/0.37	1.62/0.79	1.75/0.62	2.84/0.49	1.70/0.29
FeHfSb	3d/5d	2.91/1.52	0.91/0.33	1.67/0.71	1.51/0.89	2.52/0.63	1.51/0.38
FeVSn	3d/3d	2.13/2.67	0.85/0.74	1.45/1.42	1.52/0.94	2.20/1.33	1.32/0.80
FeNbSn	3d/4d	2.20/1.96	0.89/0.47	1.51/0.96	1.50/0.53	2.27/0.51	1.36/0.31
FeTaSn	3d/5d	2.28/1.76	0.90/0.42	1.54/0.86	1.46/0.54	2.25/0.46	1.35/0.28
CoTiSn	3d/3d	2.33/2.11	0.94/0.63	1.59/1.17	1.07/1.45	1.70/1.70	1.02/1.02
CoZrSn	3d/4d	2.12/1.45	0.96/0.38	1.57/0.75	1.48/1.25	2.32/0.94	1.39/0.56
CoHfSn	3d/5d	2.58/1.39	0.98/0.36	1.70/0.70	1.15/0.92	1.96/0.64	1.17/0.39
RhTiSn	4d/3d	2.17/1.78	0.66/0.65	1.22/1.13	0.42/1.56	0.51/1.76	0.31/1.06
IrTiSn	5d/3d	1.89/1.86	0.58/0.65	1.08/1.15	0.39/1.49	0.42/1.71	0.25/1.03
NiTiIn	3d/3d	3.09/1.47	1.05/0.61	1.88/1.03	0.62/2.52	1.17/2.60	0.70/1.56
NiZrIn	3d/4d	3.00/1.23	1.07/0.39	1.89/0.72	0.60/1.56	1.13/1.12	0.68/0.67
PdTiIn	4d/3d	2.63/1.29	0.72/0.62	1.39/1.00	0.20/2.12	0.28/2.12	0.17/1.27
PtTiIn	5d/3d	2.28/1.41	0.65/0.52	1.23/0.90	0.30/2.50	0.37/2.25	0.22/1.35
CoVSb	3d/3d	3.65/3.14	0.94/0.71	1.85/1.48	0.98/4.36	1.81/6.45	1.09/3.87
RhVSb	4d/3d	2.90/3.00	0.65/0.73	1.36/1.48	0.37/3.68	0.50/5.45	0.30/3.27
IrVSb	5d/3d	2.62/3.12	0.58/0.73	1.22/1.50	0.17/2.13	0.21/3.20	0.12/1.92
PdTiSb	4d/3d	3.31/2.58	0.74/0.62	1.54/1.26	0.29/1.84	0.45/2.32	0.27/1.39
PtTiSb	5d/3d	2.85/2.48	0.64/0.58	1.33/1.19	0.28/3.29	0.37/3.90	0.22/2.35
NiVSn	3d/3d	4.15/2.71	1.04/0.72	2.08/1.40	0.69/2.74	1.44/3.84	0.86/2.30
NiVSb	3d/3d	3.95/2.82	1.02/0.69	2.02/1.39	1.52/7.51	3.07/10.4	1.84/6.26
CuVSb	3d/3d	5.00/2.03	1.17/0.61	2.40/1.14	0.20/4.40	0.48/5.00	0.29/3.00
Gapped metals							
NiHfIn	3d/5d	3.37/1.20	1.09/0.37	1.98/0.68	0.50/1.30	0.99/0.88	0.59/0.53
CoNbSb	3d/4d	4.05/2.20	0.98/0.45	1.98/0.98	0.70/1.18	1.39/1.16	0.83/0.69
CoTaSb	3d/5d	4.08/1.93	0.98/0.39	1.99/0.86	0.56/0.76	1.11/0.65	0.67/0.39
NiTiSb	3d/3d	4.26/2.95	1.04/0.58	2.10/1.29	0.41/1.16	0.86/1.50	0.52/0.90
NiZrSb	3d/4d	4.82/1.96	1.08/0.36	2.27/0.82	0.27/0.47	0.61/0.39	0.37/0.23
NiHfSb	3d/5d	4.91/1.69	1.09/0.32	2.30/0.73	0.23/0.39	0.53/0.29	0.32/0.17
NiNbSn	3d/4d	4.72/2.19	1.09/0.46	2.25/0.99	0.62/1.30	1.40/1.29	0.84/0.77
NiTaSn	3d/5d	4.85/1.99	1.10/0.41	2.29/0.90	0.40/0.75	0.92/0.68	0.55/0.41

significant spin magnetic moments. On the other hand, the Ni/Cu atoms as well as the 4d and 5d transition metal atoms carry much smaller atomic spin magnetic moments. The spin-polarization SP at the Fermi level is defined as the difference between the number of spin-up $N^\uparrow(E_F)$ and spin-down $N^\downarrow(E_F)$ electronic states at the Fermi level divided by their sum, $SP = \frac{N^\uparrow(E_F) - N^\downarrow(E_F)}{N^\uparrow(E_F) + N^\downarrow(E_F)}$. The SP is positive in all cases and reaches an ideal 100% value when the spin-down electronic band is semiconducting. Finally, we also present the calculated Curie temperatures T_C for all spin-gapped metallic materials. For most of the compounds, T_C is larger than 200 K but does not exceed the room temperature except NiVSb and CuVSb for which it reaches a value of 670 K and 635 K, respectively. The smallest T_C value was obtained for NiZrIn which is only 5 K. Curie temperature is crucial

for applications, but our study aims to provide proof of the spin-gapless metallic concept.

The final part of our study concerns the origin of the magnetic state in the spin-gapped metals and we have gathered all related data in Table II. First, we performed non-spin polarized calculations for all compounds and computed the effective Coulomb interaction parameters U and J following the same procedure as in Ref. 44. The parameters were calculated for the valence d -electrons of the two transition metal atoms. These parameters can be used in principle to perform more elaborated electronic structure calculations accounting for the electronic correlations [54–57]. In our case these values were used to calculate the Stoner parameter as discussed in the second section. The Stoner criterion for magnetism is $I \cdot N(E_F) > 1$ where $N(E_F)$ is the number of electronic states at the Fermi level in the non-spin-polarized case.

But as stated in Ref. 47 the Stoner parameter must be multiplied by a $\alpha = 0.6$ coefficient to account for the correlation effect. Thus the Stoner criterion becomes $\alpha \cdot I \cdot N(E_F) > 1$. When this condition is met, in the scenario without spin polarization, the electronic charge at the Fermi level reaches a sufficient magnitude, prompting the compound to undergo a magnetic phase transition, thereby reducing its electronic charge at the Fermi level due to energetic favourability. If we study carefully the values in Table II, the Stoner criterion is not fulfilled for the gapped metals meaning that the non-spin-polarized state is energetically favorable. Contrary, in the case of the spin-gapped metals the Stoner criterion is fulfilled for the valence d -states of at least one of the two transition metal atoms. The strongest tendency for magnetism is exhibited by NiVSb which has also the highest Curie temperature among all studied compounds. The $\alpha \cdot I \cdot N(E_F)$ reaches a value of about 2 for the Ni-3d valence electrons and slightly larger than 6 for the V-3d valence electrons.

Summary and conclusions: Gapped metals, a newly identified category of materials, possess a band gap that falls marginally above or below the Fermi level. This unique characteristic allows them to inherently behave as p- or n-type semiconductors, eliminating the need for external doping. Inspired by this notion, we proposed the concept of "spin-gapped metals", which display intrinsic p- or n-type characteristics independently for each spin channel. Their attributes would resemble those of dilute magnetic semiconductors, obviating the need for transition metal doping. We illustrated this novel concept using semi-Heusler compounds through first-principles electronic band structure calculations. Scanning the Open Quantum Materials Database [36], we have chosen 33 semi-Heusler compounds with less or more than 18 valence electrons per unit cell since the latter are well-known semiconductors. We thoroughly examined their

electronic and magnetic attributes and have shown that 8 of them are gapped materials while the other 25 belong to this novel category of materials. The Stoner criterion can be employed to explain the occurrence of the magnetic state in these 25 Heusler compounds. Our study of these novel spin-gapped metallic materials lays the groundwork for novel technological applications of Heusler compounds.

ACKNOWLEDGMENTS

This work was supported by SFB CRC/TRR 227 of Deutsche Forschungsgemeinschaft (DFG) and by the European Union (EFRE) via Grant No: ZS/2016/06/79307, and by the Federal Ministry of Education and Research of Germany in the framework of the Palestine-German Science Bridge (BMBF grant number 01DH16027). M. T. acknowledges the TUBITAK ULAKBIM, High Performance and Grid Computing Center (TRUBA resources). B. S. acknowledges financial support from Swedish Research Council (grant no. 2022-04309). The computations were enabled in project SNIC 2021/3-38 by resources provided by the Swedish National Infrastructure for Computing (SNIC) at NSC, PDC, and HPC2N partially funded by the Swedish Research Council (Grant No. 2018-05973). B. S. acknowledges allocation of supercomputing hours by PRACE DECI-17 project "Q2Dtopomat" in Eagle supercomputer in Poland and EuroHPC resources in Karolina supercomputer in Czech Republic.

DATA AVAILABILITY STATEMENT

Data available on request from the authors

-
- [1] L. E. Bell, Cooling, heating, generating power, and recovering waste heat with thermoelectric systems, *Science* **321**, 1457 (2008).
 - [2] D. Champier, Thermoelectric generators: a review of applications, *Energy Convers. Manage* **140**, 167 (2017).
 - [3] F. Ricci, A. Dunn, A. Jain, G.-M. Rignanese, and G. Hautier, Gapped metals as thermoelectric materials revealed by high-throughput screening, *J. Mater. Chem. A*, **8**, 17579 (2020).
 - [4] O. I. Malyi and A. Zunger, False metals, real insulators, and degenerate gapped metals, *Appl. Phys. Rev.* **7**, 041310 (2020).
 - [5] M. R. Khan, H. R. Gopidi, and O. I. Malyia, Optical properties and electronic structures of intrinsic gapped metals: Inverse materials design principles for transparent conductors, *Appl. Phys. Lett.* **123**, 061101 (2023).
 - [6] K. Sato, L. Bergqvist, J. Kudrnovský, P. H. Dederichs, O. Eriksson, I. Turek, B. Sanyal, G. Bouzerar, H. Katayama-Yoshida, V. A. Dinh, T. Fukushima, H. Kizaki, and R. Zeller, First-principles theory of dilute magnetic semiconductors, *Rev. Mod. Phys.* **82**, 1633 (2010).
 - [7] B.-H. Lei and D. J. Singh, Computational search for itinerant n-type and p-type magnetic semiconductors: Arsenopyrites as bipolar magnetic semiconductors, *Phys. Rev. B* **105**, L121201 (2022).
 - [8] N. T. Tu, P. N. Hai, L. D. Anh, and M. Tanaka, (Ga,Fe)Sb: A p-type ferromagnetic semiconductor, *Appl. Phys. Lett.* **105**, 132402 (2014).
 - [9] K. Kroth, B. Balke, G. H. Fecher, V. Ksenofontov, C. Felser, and H.-J. Lin, Diluted magnetic semiconductors with high curie temperature based on C1(b) compounds: $\text{CoTi}_{1-x}\text{Fe}_x\text{Sb}$, *Appl. Phys. Lett.* **89**, 202509 (2006).
 - [10] F. Heusler, Kristallstruktur und Ferromagnetismus der Mangan-Aluminium-Kupferlegierungen, *Verh. Dtsch. Phys. Ges.* **12**, 219 (1903).
 - [11] F. Heusler and E. Take, The nature of the Heusler alloys, *Phys. Z.* **13**, 897 (1912).

- [12] T. Graf, C. Felser, and S. S. P. Parkin, Simple rules for the understanding of heusler compounds, *Progr. Sol. St. Chem.* **39**, 1 (2011).
- [13] S. Tavares, K. Yang, and M. A. Meyers, Heusler alloys: Past, properties, new alloys, and prospects, *Progr. Mat. Sci.* **132**, 101017 (2023).
- [14] S. Chatterjee, S. Chatterjee, S. Giri, and S. Majumdar, Transport properties of Heusler compounds and alloys, *J. Phys.: Condens. Matter* **34**, 013001 (2022).
- [15] I. Galanakis, Slater-pauling behavior in half-metallic heusler compounds, *Nanomaterials* **13**, 2010 (2023).
- [16] S. Ouardi, G. H. Fecher, C. Felser, and J. Kübler, Realization of spin gapless semiconductors: The Heusler compound Mn_2CoAl , *Phys. Rev. Lett.* **110**, 100401 (2013).
- [17] Q. Gao, I. Opahle, and H. Zhang, High-throughput screening for spin-gapless semiconductors in quaternary Heusler compounds, *Phys. Rev. Mater.* **3**, 024410 (2019).
- [18] I. Galanakis, K. Özdoğan, and E. Şaşıoğlu, Spin-filter and spin-gapless semiconductors: The case of Heusler compounds, *AIP Advances* **6**, 055606 (2016).
- [19] J. Ma, V. I. Hegde, K. Munira, Y. Xie, S. Keshavarz, D. T. Mildebrath, C. Wolverton, A. W. Ghosh, and W. H. Butler, Computational investigation of half-Heusler compounds for spintronics applications, *Phys. Rev. B* **95**, 024411 (2017).
- [20] M. Gilleßen and R. Dronskowski, A combinatorial study of full Heusler alloys by first-principles computational methods, *J. Comput. Chem.* **30**, 1290 (2009).
- [21] M. Gilleßen and R. Dronskowski, A combinatorial study of inverse Heusler alloys by first-principles computational methods, *J. Comput. Chem.* **31**, 612 (2010).
- [22] S. V. Faleev, Y. Ferrante, J. Jeong, M. G. Samant, B. Jones, and S. S. P. Parkin, Unified explanation of chemical ordering, the Slater-Pauling rule, and half-metallicity in full Heusler compounds, *Phys. Rev. B* **95**, 045140 (2017).
- [23] S. V. Faleev, Y. Ferrante, J. Jeong, M. G. Samant, B. Jones, and S. S. P. Parkin, Origin of the tetragonal ground state of Heusler compounds, *Phys. Rev. Appl.* **7**, 034022 (2017).
- [24] S. V. Faleev, Y. Ferrante, J. Jeong, M. G. Samant, B. Jones, and S. S. P. Parkin, Heusler compounds with perpendicular magnetic anisotropy and large tunneling magnetoresistance, *Phys. Rev. Mater.* **1**, 024402 (2017).
- [25] M. Marathe and H. C. Herper, Exploration of all-3d Heusler alloys for permanent magnets: An ab initio based high-throughput study, *Phys. Rev. B* **107**, 174402 (2023).
- [26] S. Sanvito, J. Xue, A. Tiwari, M. Zic, T. Archer, P. Toznan, M. Venkatesan, M. Coey, and S. Curtarolo, Accelerated discovery of new magnets in the Heusler alloy family, *Sci. Adv.* **3**, e1602241 (2017).
- [27] D. Jung, H.-J. Koo, and M.-H. Whangbo, Study of the 18-electron band gap and ferromagnetism in semi-heusler compounds by non-spin-polarized electronic band structure calculations, *J. Mol. Struct.:THEOCHEM* **527**, 113 (2000).
- [28] J. Pierre, R. V. Skolozdra, Y. K. Gorelenko, and M. Kouacou, From nonmagnetic semiconductor to itinerant ferromagnet in the tinisn-ticosn series, *J. Magn. Magn. Mater.* **134**, 95 (1994).
- [29] J. Tobola and J. Pierre, Electronic phase diagram of the xtz ($x=fe, co, ni$; $t=ti, v, zr, nb, mn$; $z=sn, sb$) semi-heusler compounds, *J. All. Comp.* **296**, 243 (2000).
- [30] S. Ouardi, G. H. Fecher, C. Felser, M. Schwall, S. S. Naghavi, A. Gloskovskii, B. Balke, J. Hamrle, K. Postava, J. Pištora, S. Ueda, and K. Kobayashi, Electronic structure and optical, mechanical, and transport properties of the pure, electron-doped, and hole-doped Heusler compound $CoTiSb$, *Phys. Rev. B* **86**, 045116 (2012).
- [31] M. Mokhtari, F. Dahmane, G. Benabdellah, L. Zekri, S. Benalia, and N. Zekri, Theoretical study of the structural stability, electronic and magnetic properties of xv_{sb} ($x = fe, co, and ni$) half-heusler compounds, *Condens. Matter Phys.* **11**, 43705 (2018).
- [32] E. Gürbüz, S. Ghosh, E. Şaşıoğlu, I. Galanakis, I. Mertig, and B. Sanyal, Spin-polarized two-dimensional electron/hole gas at the interface of nonmagnetic semiconducting half-Heusler compounds: Modified Slater-Pauling rule for half-metallicity at the interface, *Phys. Rev. Materials* **7**, 054405 (2023).
- [33] E. Gürbüz, M. Tas, E. Şaşıoğlu, I. Mertig, B. Sanyal, and I. Galanakis, First-principles prediction of energy bandgaps in 18-valence electron semiconducting half-Heusler compounds: Exploring the role of exchange and correlation, *J. Appl. Phys.* **134**, 205703 (2023).
- [34] K. Xia, C. Hu, C. Fu, X. Zhao, and T. Zhu, Half-Heusler thermoelectric materials, *Appl. Phys. Lett.* **118**, 140503 (2021).
- [35] X. Ti, J. Zhu, S. Guo, J. Li, X. Liu, and Y. Zhang, Bonding properties of Rubik's-cube-like Slater-Pauling Heusler semiconductors for thermoelectrics, *Phys. Rev. B* **108**, 195203 (2023).
- [36] <https://oqmd.org/> .
- [37] J. P. Perdew, K. Burke, and M. Ernzerhof, Generalized gradient approximation made simple, *Phys. Rev. Lett.* **77**, 3865 (1996).
- [38] S. Smidstrup, D. Stradi, J. Wellendorff, P. A. Khomyakov, U. G. Vej-Hansen, M.-E. Lee, T. Ghosh, E. Jónsson, H. Jónsson, and K. Stokbro, First-principles Green's-function method for surface calculations: A pseudopotential localized basis set approach, *Phys. Rev. B* **96**, 195309 (2017).
- [39] S. Smidstrup, T. Markussen, P. Vancaeyveld, J. Wellendorff, J. Schneider, T. Gunst, B. Verstichel, D. Stradi, P. A. Khomyakov, U. G. Vej-Hansen, M.-E. Lee, S. T. Chill, F. Rasmussen, G. Penazzi, F. Corsetti, A. Ojanpera, K. Jensen, M. L. N. Palsgaard, U. Martinez, A. Blom, M. Brandbyge, and K. Stokbro, QuantumATK: an integrated platform of electronic and atomic-scale modelling tools, *J. Phys.: Condens. Matter* **32**, 015901 (2020).
- [40] M. J. van Setten, M. Giantomassi, E. Bousquet, M. J. Verstraete, D. R. Hamann, X. Gonze, and G. M. Rignanese, The PSEUDODOJO: Training and grading a 85 element optimized norm-conserving pseudopotential table, *Comp. Phys. Commun.* **226**, 39 (2018).
- [41] M. Meinert, Modified Becke-Johnson potential investigation of half-metallic Heusler compounds, *Phys. Rev. B* **87**, 045103 (2013).
- [42] H. J. Monkhorst and J. D. Pack, Special points for Brillouin-zone integrations, *Phys. Rev. B* **13**, 5188 (1976).
- [43] E. Şaşıoğlu, I. Galanakis, F. Friedrich, and S. Blügel, Ab initio calculation of the effective on-site Coulomb interaction parameters for half-metallic magnets, *Phys. Rev. B* **88**, 134402 (2013).

- [44] M. Tas, E. Şaşıoğlu, S. Blügel, I. Mertig, and I. Galanakis, Ab initio calculation of the hubbard u and hund exchange j in local moment magnets: The case of Mn-based full Heusler compounds, *Phys. Rev. Mater.* **6**, 114401 (2022).
- [45] <http://www.flapw.de>.
- [46] C. Friedrich, S. Blügel, and A. Schindlmayr, Efficient implementation of the GW approximation within the all-electron FLAPW method, *Phys. Rev. B* **81**, 125102 (2010).
- [47] G. Stollhoff, A. M. Oles, and V. Heine, Stoner exchange interaction in transition metals, *Phys. Rev. B* **41**, 7028 (1990).
- [48] A. Jakobsson, P. Mavropoulos, E. Şaşıoğlu, S. Blügel, M. Ležaić, B. Sanyal, and I. Galanakis, First-principles calculations of exchange interactions, spin waves, and temperature dependence of magnetization in inverse-Heusler-based spin gapless semiconductors, *Phys. Rev. B* **91**, 174439 (2015).
- [49] A. I. Liechtenstein, M. I. Katsnelson, V. P. Antropov, and V. A. Gubanov, Local spin density functional approach to the theory of exchange interactions in ferromagnetic metals and alloys, *J. Magn. Magn. Mater.* **67**, 65 (1987).
- [50] J. M. Wills, M. Alouani, P. Andersson, A. Delin, O. Eriksson, and O. Grechnyev, *Full-Potential Electronic Structure Method: Energy and Force Calculations With Density Functional and Dynamical Mean Field Theory*, Springer Series in Solid-State Sciences, Vol. 167 (Springer, 2010).
- [51] Q. Gao, I. Opahle, and H. Zhang, High-throughput screening for spin-gapless semiconductors in quaternary heusler compounds, *Phys. Rev. Mater.* **3**, 024410 (2019).
- [52] T. Aull, E. Şaşıoğlu, I. V. Maznichenko, S. Ostanin, A. Ernst, I. Mertig, and I. Galanakis, Ab initio design of quaternary Heusler compounds for reconfigurable magnetic tunnel diodes and transistors, *Phys. Rev. Mater.* **3**, 124415 (2019).
- [53] K. Özdoğan, E. Şaşıoğlu, and I. Galanakis, Slater-Pauling behavior in LiMgPdSn-type multifunctional quaternary Heusler materials: Half-metallicity, spin-gapless and magnetic semiconductors, *J. Appl. Phys.* **113**, 193903 (2013).
- [54] K. Karlsson, F. Aryasetiawan, and O. Jepsen, Method for calculating the electronic structure of correlated materials from a truly first-principles LDA+ U scheme, *Phys. Rev. B* **81**, 245113 (2010).
- [55] I. Solovyev, Combining DFT and many-body methods to understand correlated materials, *J. Phys.: Condens. Matter* **20**, 293201 (2008).
- [56] J. Minár, Correlation effects in transition metals and their alloys studied using the fully self-consistent KKR-based LSDA + DMFT scheme, *J. Phys.: Condens. Matter* **23**, 253201 (2011).
- [57] F. Lechermann, A. Georges, A. Poteryaev, S. Biermann, M. Posternak, A. Yamasaki, and O. K. Andersen, Dynamical mean-field theory using Wannier functions: A flexible route to electronic structure calculations of strongly correlated materials, *Phys. Rev. B* **74**, 125120 (2006).
- [58] G. Xu, E. K. Liu, Y. Du, G. J. Li, G. D. Liu, W. H. Wang, and G. H. Wu, New spin gapless semiconductors family: Quaternary heusler compounds, *Europhys. Lett.* **102**, 17007 (2013).